Seasonal Diagnostic and Predictability of Rainfall in Subtropical South America Based on Tropical Pacific SST

ALDO MONTECINOS

Departamento de Geofísica, Universidad de Chile, Santiago, Chile

ALVARO DÍAZ

Instituto de Mecánica de los Fluídos e Ingeniería Ambiental, Universidad de la República, Montevideo, Uruguay

PATRICIO ACEITUNO

Departamento de Geofísica, Universidad de Chile, Santiago, Chile

(Manuscript received 5 October 1998, in final form 21 April 1999)

ABSTRACT

The seasonality of the simultaneous relationship between tropical Pacific SST and rainfall, as well as rainfall predictability one season in advance in subtropical South America (25°–40°S), is studied using different multivariate techniques. This study shows that ENSO-related rainfall anomalies in subtropical South America are restricted mostly to regions on the eastern and western sides of the continent and mainly during the second half of the year. The relationship is almost exclusively of the warm–wet/cold–dry type, but a more widespread impact is found when anomalously warm conditions prevail in the equatorial Pacific. A spatially coherent region with a significant warm–wet/cold–dry signal is detected in southeastern South America during austral spring (October–November), including southern Brazil, southern Paraguay, Uruguay, and eastern Argentina. This signal moves inland toward the west from spring to early summer. During late winter (July–August), a similar SST–rainfall relationship is found in subtropical Chile and southern Brazil. In Chile, a southward propagation of the signal is observed from winter to spring.

Most significant ENSO-related rainfall anomalies seem to occur after the maximum in the precipitation annual cycle. The combined analysis of seasonal diagnostics and predictability of rainfall show that the seasonal rainfall predictability in subtropical South America based on tropical Pacific SST to a greater extent is restricted to a specific time of the year and regions that broadly coincide with those where the simultaneous SST–rainfall relationship is significant. This fact suggests that persistence of tropical Pacific SST anomaly is the major source of seasonal rainfall predictability in this region, when SST is used as a predictor.

1. Introduction

The economy of subtropical South America is strongly based on agriculture. Furthermore, production of hydroelectric power within this region is essential to satisfy an ever-increasing energy demand. Both of these activities, as well as many others that depend on water resources, are strongly affected by the occurrence of anomalously wet or dry climate conditions. Thus, a better understanding of the variability and predictability of the precipitation regime is of primary importance. The objectives of this study concerning precipitation in this region are twofold: 1) to analyze the simultaneous relationship between anomalous rainfall in the region and sea surface temperature (SST) anomalies in the tropical Pacific on the seasonal timescale, focusing on the occurrence of anomalously dry and wet conditions during Pacific warm and cold episodes; and 2) to assess the predictability of seasonal rainfall using SST in the tropical Pacific as a predictor.

The seasonal changes of simultaneous and lagged SST–rainfall relationships are studied on a bimonthly basis. The intraseasonal variability in the atmospheric circulation may explain the occurrence of monthly rainfall anomalies that are opposite in sign to those typically observed during the ENSO phenomenon (see, e.g., Rutllant and Fuenzalida 1991). Application of bimonthly averages aims to filter the intraseasonal and shorter timescale variability while still allowing for a proper representation of the seasonality in the SST–rainfall relationship.

Figure 1 shows the characteristics of the rainfall annual cycle in subtropical South America, using long-

Corresponding author address: Aldo Montecinos, Departamento de Geofísica, Universidad de Chile, Casilla 2777, Santiago, Chile.
E-mail: amonteci@dgf.uchile.cl

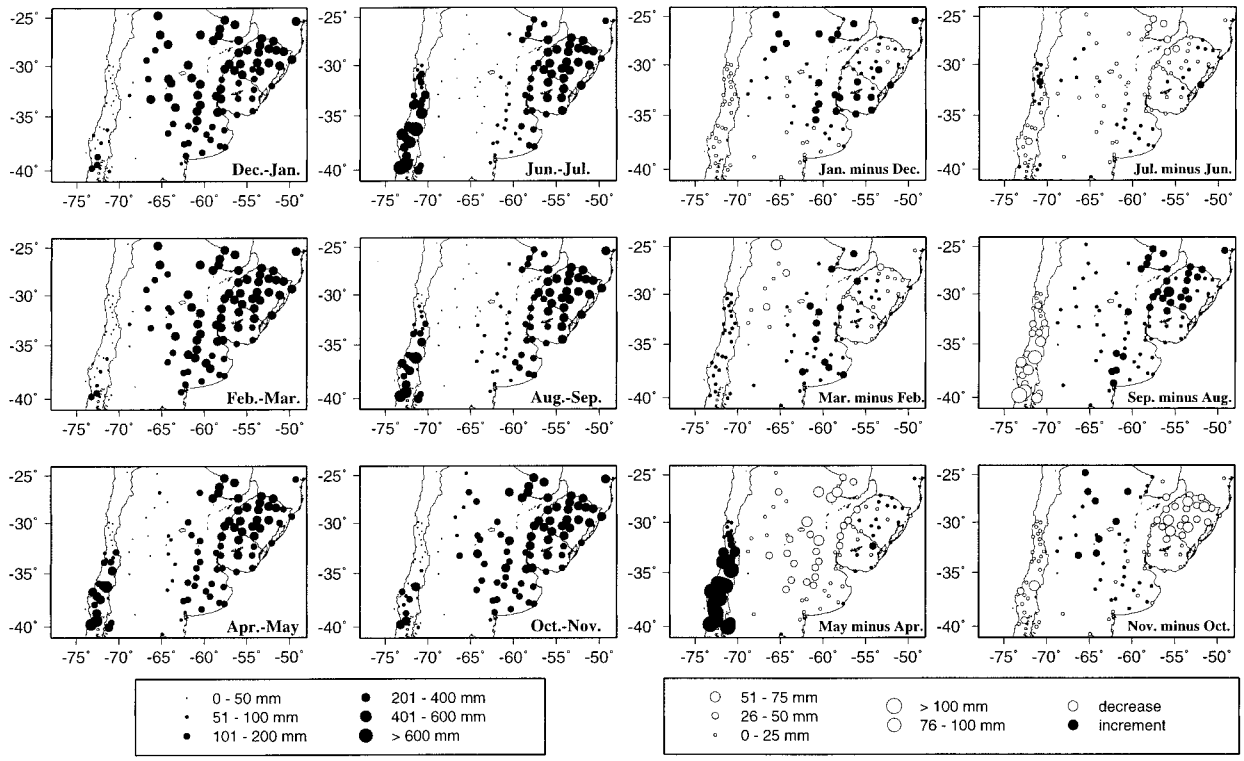

FIG. 1. Bimonthly rainfall climatology (left panels) during 1947–86, and monthly differences during each bimonthly interval (right panels): Jan–Feb, Mar–Apr, May–Jun, Jul–Aug, Sep–Oct, Nov–Dec. Symbols are described at the bottom of the figure.

term averages and rainfall changes during nonoverlapping bimonthly intervals. Four sectors with rainfall having a relatively homogeneous annual cycle are identified: the Pacific coastal band (central Chile), the continental strip on the east side of the Andes (70°–65°W), the central continental strip (65°–60°W), and the Atlantic band east of 60°W.

1) Pacific band (central Chile): This sector corresponds to the narrow continental strip between the Pacific coast and the Andes Mountains. There is a well-defined contrast between the extreme and permanent arid conditions prevailing in the northern sector and the wetter conditions in the south. Although there is some increase in rainfall from February to March, the largest seasonal increase occurs between April and May. From June to July the change in rainfall is relatively small, although a slight increase is observed northward of approximately 33°S and a decrease in the region to the south of this latitude. The significant decrease in rainfall during August–September indicates the end of the wet season.
2) Continental strip eastward from the Andes (70°–65°W): The region east of the Andes is relatively dry. This is partially due to the rain shadow effect of the Andes, associated with the midlatitude westerly flow. The meridional variation of rainfall and its seasonality are broadly opposite to those described for Chile. Accordingly, Fig. 1 shows that rainfall increases from September to January. In the southern portion of this region, relatively dry conditions prevail throughout the year (average rainfall less than 50 mm in each bimonthly period).
3) Central continental strip (65°–60°W): Here, the annual cycle of rainfall is characterized by a minimum during winter (May–August) and a maximum during summer and early fall (January–April). The slow increase in rainfall observed during the summer semester ends in March and it is followed by a relatively fast decrease during April and May.
4) Atlantic band east of 60°W: This region includes the southern part of Paraguay, southern Brazil, Uruguay, and the pampas sector of eastern Argentina. Although precipitation is larger in the northern sector, the entire region is characterized by a relatively flat annual cycle with bimonthly rainfall exceeding 100 mm during the entire year. The seasonal changes in rainfall show some distinct features, such as the relatively large increase during the transition from winter to spring (August–September) in the northern sector of the region (southern Brazil, southern Paraguay, and northeastern Argentina), which is followed by a decrease during spring (October–November), in contrast with the overall increase observed elsewhere in Argentina.

Several studies support the existence of links between the Southern Oscillation (and associated SST anomalies

in the tropical Pacific) with precipitation anomalies in subtropical South America.

A warm–wet/cold–dry relationship has been documented for central Chile during austral winter (Rubin 1955; Pittock 1980; Quinn and Neal 1983; Aceituno 1988; Kiladis and Díaz 1989). Rubin (1955) documented a tendency for below-normal precipitation in central Chile when the subtropical anticyclone in the southeastern Pacific is anomalously intense during the positive phase of the Southern Oscillation. Rutllant and Fuenzalida (1991) confirmed the warm–wet/cold–dry tendency, pointing out that major winter storms associated with warm events are related to blocking in the Bellingshausen Sea area (90°W). They also called the attention to the occurrence of dry months during wet winters in El Niño years, interpreting this as the effect of intraseasonal variability characterized by alternating circulation anomaly patterns at subtropical latitudes.

Pittock (1980) documents the existence of a significant negative correlation between the Southern Oscillation index (SOI) and precipitation over eastern Argentina during spring. For southeastern South America, which includes southern Brazil, Uruguay, and part of northeastern Argentina, Ropelewski and Halpert (1987, 1989) documented a clear tendency for enhanced precipitation during spring and summer during El Niño years, and a tendency for below-normal precipitation during high SOI years, between June and December. This results have been confirmed by Pisciottano et al. (1994) for Uruguay and Grimm et al. (1998) for southern Brazil. Moreover, Pisciottano et al. (1994) found that during El Niño (La Niña) events there is a tendency to have higher (lower) than average rainfall from March to July (year +1). Díaz et al. (1998) show that both Pacific and Atlantic SST anomalies influence the rainfall regime in Uruguay and southern Brazil (state of Rio Grande do Sul) during austral spring and summer, although during the fall–winter period (April–July) only the SST anomalies in the southwestern Atlantic seem to have an influence on rainfall anomalies in this region.

Descriptions of precipitation and SST data and their preprocessing are found in section 2. Sections 3 and 4 outline the analysis techniques and document the seasonality and spatial characteristics of the simultaneous SST–rainfall relationship, and of the seasonal rainfall predictability based on tropical Pacific SST. Finally, section 5 contains the most relevant results and conclusions.

2. Data

a. Precipitation

The main rainfall dataset for this study includes monthly totals from 106 stations in the subtropical sector of South America (25°–40°S) covering the period December 1946–December 1986. To assess the stability of some results, a second dataset with monthly rainfall values from 79 stations during the period December 1918–December 1989 was used. Most of the rainfall records are complete, while those that are not have less than 5% of missing data.

This dataset was compiled by Servicio Meteorológico Nacional (Argentina), Dirección Meteorológica de Chile (Chile), Dirección General de Aguas (Chile), Instituto de Pesquisas Agronómicas do Rio Grande do Sul (Brazil), Instituto Nacional de Meteorología (Brazil), Dirección Nacional de Meteorología (Uruguay), and Dirección de Meteorología (Paraguay). The data was provided by 46 stations in Argentina, 25 in Chile, 21 in southern Brazil (state of Rio Grande do Sul), 11 in Uruguay, and 3 in southern Paraguay. No rainfall data were considered for the arid region of northern Chile. Indeed, data coverage is relatively poor in Paraguay, the state of Santa Catarina in southern Brazil, and in northern and southern Argentina.

b. Sea surface temperature

For the period 1946–81 monthly mean values of SST were obtained from the Global Ocean–Global Atmosphere dataset. This is an analysis of the Comprehensive Ocean Atmosphere Data Set produced at the Geophysical Fluid Dynamics Laboratory (Lau and Nath 1994). SST data, which are available on a grid with a 4.5° × 7.5° lat–long resolution, were extracted for the 244 grid points in the region 20°N–40°S, 150°E–80°W. For the period 1982–86, monthly mean values corresponding to the optimum interpolation SST data (Reynolds and Smith 1994) were used. This SST dataset, which is available at a 1° × 1° lat–long resolution, was interpolated to the 4.5° × 7.5° lat–long grid using a cubic interpolation method.

The average SST anomaly in the Niño-3 region (5°N–5°S and 150°–90°W) was taken as an index for the SST conditions along the equatorial Pacific during the period 1950–89. For the period December 1918–December 1949 the monthly time series of SST anomalies, calculated by Wright (1989), was used for the region defined by 6°–2°N, 170°–90°W; 2°N–6°S, 180°–90°W; 6°–10°S, 150°–110°W.

c. Data preprocessing

Bimonthly SST anomalies were calculated at each grid point by subtracting the long-term mean from individual bimonthly averages. Time series of accumulated bimonthly rainfall were calculated at each station. The first bimonthly interval is December 1946–January 1947 and the last is November–December 1986. These procedures yield twelve bimonthly time series (each 40 yr long) for each field. For the sake of simplicity bimonthly periods will be usually referred to as DJ, JF, FM, MA, AM, MJ, JJ, JA, AS, SO, ON, and ND.

TABLE 1. Explained variance (%) by the first principal component of Pacific SST anomaly in the region 20°N–40°S, 150°E–80°W, for each of 12 sliding bimonthly intervals: Jan–Feb, Feb–Mar up to Dec–Jan.

Months	JF	FM	MA	AM	MJ	JJ	JA	AS	SO	ON	ND	DJ
Variance (%)	36.8	31.0	27.5	28.5	32.3	34.3	36.0	40.6	44.7	46.8	46.2	42.0

3. Simultaneous relationship between SST and precipitation

The simultaneous relationship between SST in the tropical Pacific and precipitation in subtropical South America is investigated using two different techniques. First, the linear relationship between the first principal component of the SST field and rainfall at individual stations is evaluated using correlation analysis. In the second approach, the rainfall anomalies during extreme warm and cold conditions in the central equatorial Pacific are studied through a stratification procedure. Considering the strong seasonality of the rainfall regime in certain regions (Fig. 1) for a particular bimonthly period, those stations having at least one-third of the record with zero precipitation were excluded from both analyses.

a. Correlation analysis

Principal component analysis was applied to bimonthly fields of Pacific SST in the region 20°N–40°S, 150°E–80°W. The dominant first component captures most of the interannual variability related to ENSO, although the percentage of the explained variance has a strong seasonality (Table 1), with the minimum value in fall (27% in MA) and maximum in spring (47% in ON). In fact, the SST index built by combining the PC1s calculated for bimonthly intervals has a strong correlation with the Niño-3 series of SST anomaly, and its periods of anomalously high and low values (Fig. 2a) very closely coincide with the timing of El Niño and La Niña episodes in the equatorial Pacific, according to Trenberth (1997). Moreover, the pattern of correlation between the spatially integrated SST index formed with the bimonthly PC1s and the actual SST anomalies at grid points (Fig. 2b) also has a close resemblance to the composite SST anomaly pattern described by Rasmusson and Carpenter (1982) for the transition and mature phases of the El Niño phenomenon.

For each bimonthly period the correlation between the PC1 and rainfall at individual stations was calculated. According to a standard Student's t-test, correlations larger than 0.5 in magnitude are highly significant (at a 0.2% level), while those larger than 0.3 in magnitude are significant at the 6% level. To obtain a global measure of the linear relationship between PC1 and precipitation, the percentage of rainfall stations having significant positive correlations was calculated for each bimonthly interval (Table 2). This percentage is maximum during the austral spring (72% in ND and 63% in ON) and minimum during austral fall (2% in MA and 4% in AM), which coincides with the periods of the year when the percentage of SST variance explained by the first principal component is highest and lowest in the annual cycle, respectively (see Table 1). Overall, Table 2 indicates that the tropical Pacific SST plays a relatively larger role in modulating interannual rainfall variability in subtropical South America during the second semester of the year, especially during late spring (October–December). The seasonality in the percentage of significant negative correlations is not shown as the warm–wet/cold–dry relationships are strongly prevalent in this part of South America.

Bimonthly patterns of the correlation between PC1 and rainfall are presented in Fig. 3. The correlation method was not applied at stations where the dry season is characterized by the total absence of rainfall, as in Chile (30°–35°S) during the summer semester (October–March).

During the austral summer, weak negative correlations appear in central–southern Chile and adjacent stations in Argentina. In DJ positive significant values are predominantly located along a longitudinal band identified as the central continental strip. Later on, from JF to AM, few stations show significant correlations. In MJ, a weak signal appears in central Chile; this signal enhances during JJ when significant positive correlations appear from 30° to 34°S. In JA, the region with positive significant values in Chile extends southward to 37°S and the same signal appears at stations in the northern part of Rio Grande do Sul (26°–30°S).

From AS to DJ, highly significant correlations (i.e., larger than 0.5) appear in all bimonthly periods, but they are mostly concentrated in Chile and along the eastern part of subtropical South America. In Chile, the pattern described for JA strengthens during AS, although a weakening in the magnitude of positive correlations are apparent in the northern sector. In SO, the signal in Chile weakens in the northern sector and enhances farther south, reaching the southernmost position during ON. From AS to ND, positive correlations prevail along the eastern part of subtropical South America. The values are highly significant during ON, especially in southern Brazil, northern Uruguay, and northeastern Argentina. During ND this pattern of positive correlation weakens in the northeast and shifts westward. This process continues in DJ, with the correlation pattern described previously for this bimonthly interval.

b. Stratification analysis

The SST–rainfall relationship during warm and cold conditions in the equatorial Pacific was analyzed on a

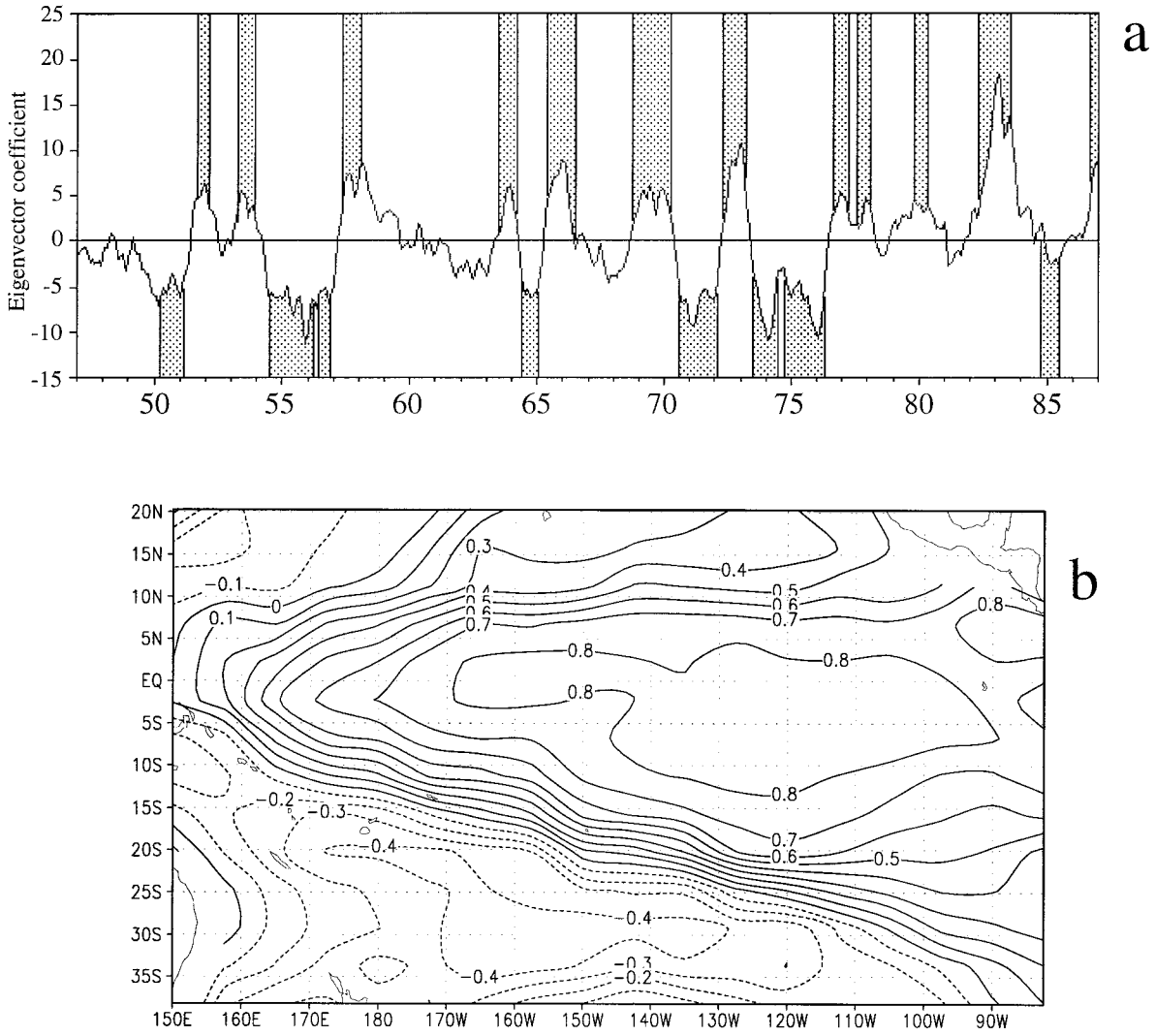

FIG. 2. (a) Combined SST PC1 time series from Dec 1946–Jan 1947 to Nov–Dec 1986. Warm and cold periods in the equatorial Pacific according to Trenberth (1997) are indicated. (b) Correlation scores between combined SST PC1 and SST anomaly considering all bimonthly intervals in the period 1947–86.

bimonthly basis using a stratification technique. This procedure differs from those performed on an annual basis, using El Niño and La Niña years as indicators of warm and cold conditions (i.e., Ropelewski and Halpert 1987, 1989). Here, anomalously warm and cold conditions were identified on a bimonthly basis as those when the central equatorial Pacific SST is in the highest and lowest 20% of the empirical distribution during the period 1947–86. In this way, eight warm and eight cold cases were identified for each bimonthly interval. It should be noted that only 40% of the years are considered in this analysis, as the methodology does not address the SST–rainfall relationship when the SST anomaly is in the range between the 20th and 80th percentiles.

The warm and cold bimonthly intervals defined by this stratification procedure broadly coincide with the periods defined by Trenberth (1997) as El Niño and La Niña events during the period 1950–86. Specifically, 90% of the warm intervals are part of El Niño events and 80% of the cold intervals belong to La Niña epi-

TABLE 2. Percentage of stations having significant positive correlation between SST PC1 and precipitation in subtropical South America, during 1947–86, for each of the 12 sliding bimonthly intervals: Jan–Feb, Feb–Mar up to Dec–Jan.

Months	JF	FM	MA	AM	MJ	JJ	JA	AS	SO	ON	ND	DJ
%	7.7	6.6	2.0	3.8	7.6	13.2	27.3	21.9	21.0	63.0	71.9	17.6

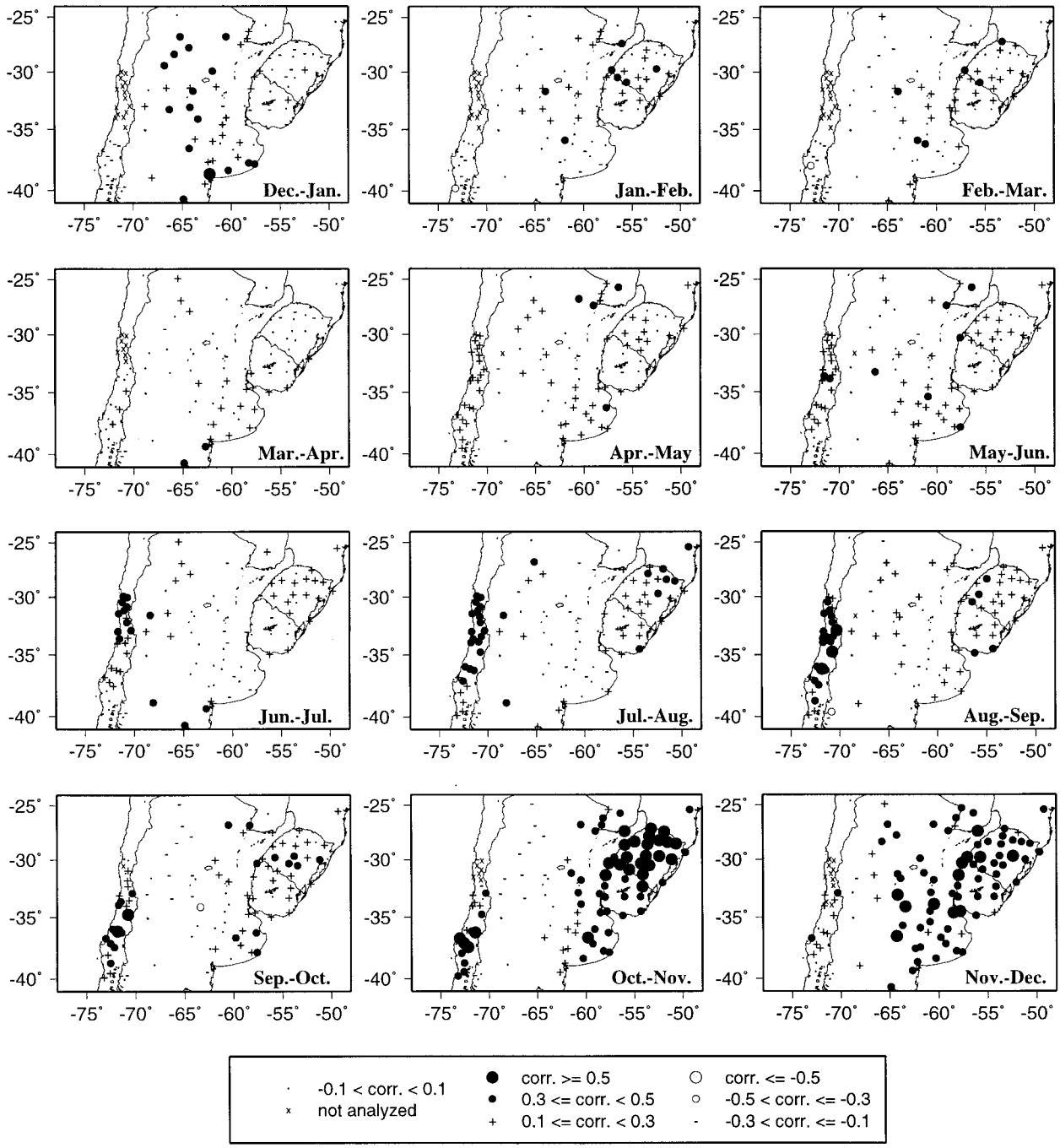

FIG. 3. Pattern of correlation between SST PC1 and rainfall for each of the 12 sliding bimonthly intervals: Dec–Jan, Jan–Feb, Feb–Mar, up to Nov–Dec. Symbols indicate magnitude and sign of correlation (see code in the figure). A magnitude larger than 0.30 is significant at the 6% level.

sodes. In both cases most of the discrepancies are observed during the first half of the year. It is also found that during 1962, 1963, 1967, and 1968 the stratification technique identifies cold bimonthly intervals that were not part of La Niña periods as defined by Trenberth (1997). There are also intervals that coincide with El Niño and La Niña events, but since the associated SST anomalies are not in the extreme 20th percentile, our methodology does not consider them as warm and cold cases.

Limits of the 20th and 80th percentiles of the empirical distribution of SST anomaly in the equatorial Pacific (Table 3) have a seasonality similar to that of the variance explained by the SST PC1 (Table 1). The

TABLE 3. Central equatorial Pacific SST anomalies (in °C) defining limits of the (a) highest and (b) lowest 20% of its empirical distribution, and (c) standard deviation of SST anomaly, for each of the 12 sliding bimonthly intervals: Jan–Feb, Feb–Mar up to Dec–Jan.

Months	JF	FM	MA	AM	MJ	JJ	JA	AS	SO	ON	ND	DJ
Highest 20% (a)	0.64	0.45	0.38	0.56	0.56	0.74	0.89	0.89	0.91	1.04	1.08	0.91
Lowest 20% (b)	−0.58	−0.38	−0.48	−0.47	−0.60	−0.60	−0.56	−0.73	−0.68	−0.76	−0.94	−0.72
Std dev (c)	0.86	0.64	0.54	0.63	0.72	0.72	0.77	0.80	0.87	0.98	1.09	1.05

largest span between both percentiles is observed in November–December when the 20th and 80th percentiles correspond to −1.0° and +1.0°C, approximately. The much lower interannual SST variance during fall (March–April) explains the relatively small SST anomalies corresponding to those percentiles (−0.5° and +0.4°C, approximately).

In regards to rainfall, accumulated bimonthly values at each station were classified in dry, normal, and wet categories, using terciles of the empirical distribution as a classification rule. Then, for each bimonthly period the frequency of each category was determined for the eight warm and eight cold years selected with the SST stratification procedure. Three possible conclusions may arise, namely, the existence of a shift in the rainfall distribution toward the wet or toward the dry categories, or the absence of a clear deviation.

It is particularly relevant to examine the occurrence (or absence) of extreme categories (dry and wet) when anomalous warm or cold conditions prevail in the Pacific. Then, the frequency of their occurrences are examined and tested using an hypergeometric distribution (Feller 1957). According to this test, the occurrence of at least five cases belonging to one of the extreme categories (wet or dry) in the sample of eight warm (or cold) cases is statistically significant (5.7% level). These cases are called category-1 significant. Furthermore, the absence of one of the extreme categories (wet or dry) in those samples is highly significant (2.9% level). These cases, are called category-2 significant.

Wetness and dryness indices were defined to characterize statistically significant results for category 1 or 2. When both are fulfilled, it will be said that the station belongs to W1 or D1 class, depending on whether wet or dry category is the predominant one. When the relationship is only category-1 significant, it will be said that the station belongs to the W2 or D2 class (depending if dominant categories are wet or dry). The rare cases of five occurrences in one extreme tercile and three in the opposite one were not considered in this classification, as it was subjectively considered that there is not a clear tendency for wet or dry conditions in this case. Finally, when the relationship is only category-2 significant, the station will be classified as NtD (not dry) or NtW (not wet). Excluded from this classification were the few cases when either the dry or wet category was not observed but the most frequent category was the normal one (five or more cases out of eight). The analysis described was performed at stations having at most one-third of the record with zero values for each bimonthly interval. In order to simplify, stations belonging to the W1 class will be designated as W1 stations, etc.

Spatial patterns of wetness and dryness indices when anomalously warm conditions prevail in the central equatorial Pacific are shown in Fig. 4. Classes W1, W2, and NtD are predominant, indicating that anomalously high SST is primarily associated with abundant rainfall or at least not dry conditions. This will be liberally designated as a warm–wet relationship.

The strongest, long-lasting, and spatially coherent warm–wet signal is observed from midspring to midsummer (October–January). During ON, most of the W1 and W2 cases concentrate along the Atlantic band (northern Uruguay, southern Brazil, southern Paraguay, and the Buenos Aires province), and in central–southern Chile (36°–39°S), where this period coincides with the end of the wet season. In ND, the warm–wet signal weakens in Chile but it gets stronger in southern Brazil and Uruguay (with some changes in the spatial distribution of classes W1 and W2). During this bimonthly period, the warm–wet relationship shifts toward southeastern Argentina. In DJ, the signal appears essentially at stations along a longitudinal band (around 63°W) between 30° and 41°S, and in the border between Uruguay and Brazil.

In JF, a warm–wet signal (class W2) is apparent in northwestern Uruguay, northern and western Rio Grande do Sul (southern Brazil), and southern Paraguay. This period is also characterized by a tendency for relatively dry conditions in central–southern Chile (class D2), where rainfall is at its minimum in the annual cycle. This warm–dry relationship gets stronger during FM in the same region, when D1 category is predominant. In MA another warm–dry signal appears in northern and eastern Uruguay and in some stations in Argentina. From MA to MJ the patterns of rainfall anomalies do not show a consistent evolution in time, suggesting that the SST–rainfall relationship during fall is relatively weak.

Another intense warm–wet signal, with clear seasonality and spatial coherence, appears in Chile during winter. In JJ, the W2 index is predominant from 30° to 35°S, while in the rest of the subtropical domain the rainfall regime seems not to be affected by the occurrence of anomalously warm conditions in the central Pacific. The warm–wet signal in Chile gets stronger in JA as the W2 index predominates in the band 30°–40°S. The same type of signal is also observed in southern Brazil during

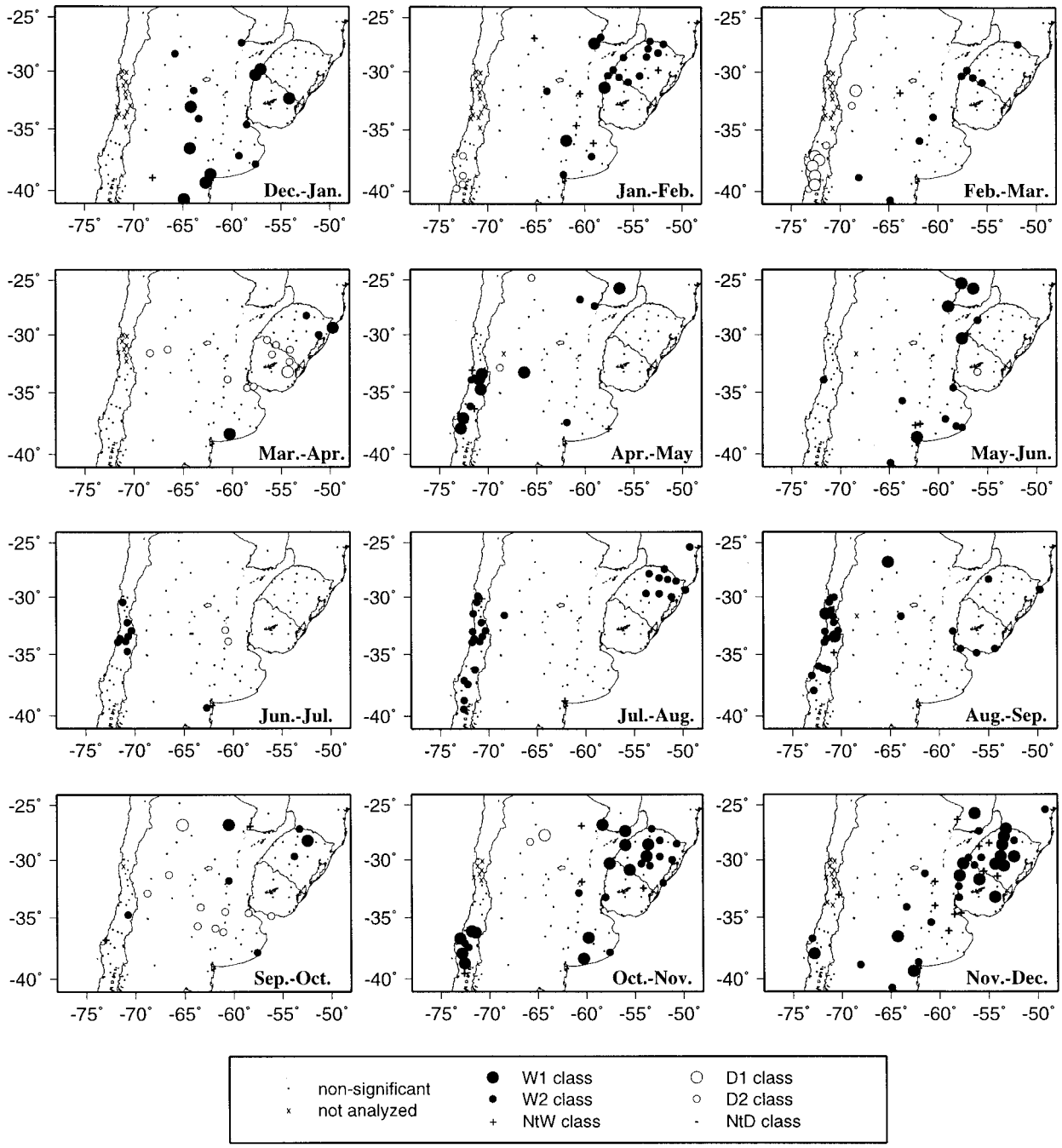

FIG. 4. Wetness and dryness classes obtained by stratification analysis considering warm cases, for each of the 12 sliding bimonthly periods: DJ, JF, FM, up to ND. Class symbols are included on the bottom of the figure.

this bimonthly interval, but it disappears during AS. In Chile, the tendency for anomalously wet conditions seems stronger in AS, when the rainfall is decreasing in the annual cycle (Fig. 1).

The results of stratification analysis for anomalously cold conditions in the central equatorial Pacific (Fig. 5) reveal a relatively weak rainfall–SST relationship. Specifically, during the first semester of the year (DJ–MJ bimonthly intervals), only in northern central Chile is a weak tendency for anomalously dry conditions during the onset of the rainy season (AM) observed. In Chile, the most significant features during the second semester of the year is the tendency for below-normal rainfall (or at least not wet conditions) in northern central sector (30°–35°S) at the height of the rainy season (JJ), and more to the south (33°–37°S) during the spring (SO).

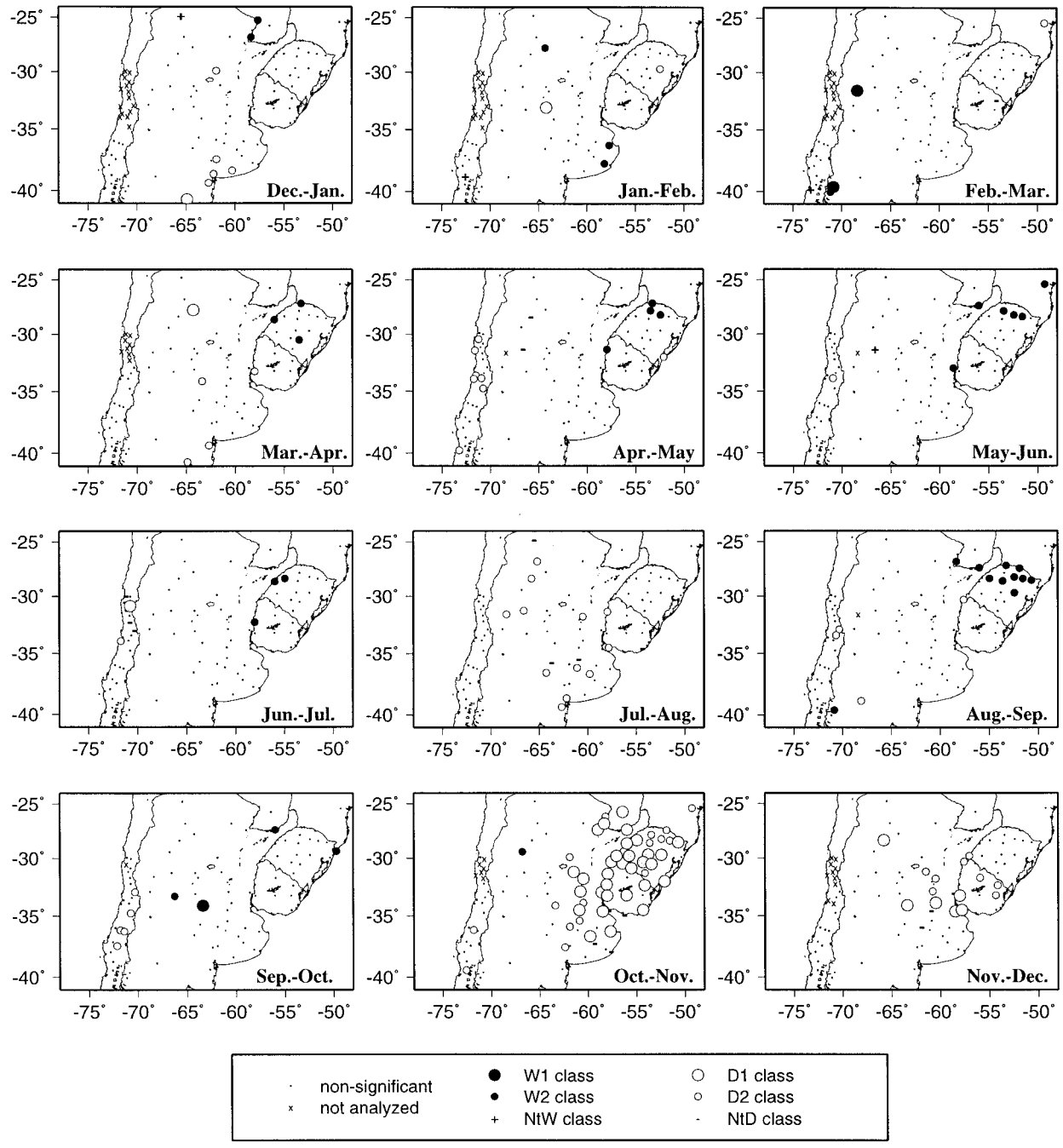

FIG. 5. As in Fig. 4, but for cold cases.

On the east side of the Andes, the largest and most coherent cold–dry relationship appears over the entire eastern sector of subtropical South America during ON, and to a lesser extent during ND when the signal remains in the region between 30° and 35°S and from 65°W eastward.

It is interesting to note that rainfall anomalies during warm and cold cases are broadly opposite in central Chile during winter and over the northeastern sector of the subtropical domain during the spring. In some cases this symmetric behavior does not hold, as is the case in southern–central Chile during the summer and early fall when the tendency for below-normal rainfall during El Niño conditions (Fig. 4, JF and FM) does not have a counterpart of opposite rainfall anomalies during La Niña (Fig. 5, JF and FM). Even more unexpected is the situation in the northeastern sector of the region, where a tendency for rather wet conditions is observed during

warm and cold cases in the austral winter and early spring (see JA in Fig. 4 and AS in Fig. 5).

To examine the influence of differences in temporal smoothing of SST and rainfall data, the stratification analyses, whose results are presented in Figs. 4 and 5, were repeated using trimesters instead of bimonthly intervals (not shown here). No major discrepancies were detected.

In order to assess the stability of results obtained with the bimonthly stratification, the procedure was repeated over a longer period (1919–89) but considering only 79 rainfall stations. The spatial distribution of wetness and dryness categories for warm and cold cases (not shown here) are fairly similar to those depicted in Figs. 4 and 5. Most differences are in the frequency of the extreme categories (wet or dry), but not in the shift toward wet or dry conditions. The main differences in comparing the longer record to the shorter record appear for the warm cases. The most relevant are (a) the stronger tendency for a rainfall deficit in Chile during JF, (b) a weaker warm–dry relationship for the eastern sector during MA, (c) a stronger warm–wet signal in eastern and central Argentina and a weaker signal in Paraguay in MJ, and (d) a tendency for wet conditions in Chile to extend to the central–southern portion of the continent in JJ.

For the cold cases, the main differences appear in JJ, SO, ND, and DJ when the patterns of a cold–dry relationship for the longer period cover a broader area, and the signals are stronger compared with those in Fig. 5.

A similar stratification analysis (not shown here) was performed for the bimonthly intervals not considered in the extreme cases, corresponding to the 60% of the SST anomaly distribution between the 20th and 80th percentiles. In all bimonthly intervals, the frequency of dry, normal, and wet categories are not significantly different from those observed in the climatological distribution.

4. Seasonal predictability

Canonical correlation analysis (CCA) was used to evaluate the seasonal rainfall predictability in subtropical South America when tropical Pacific SST is used as a predictor. CCA is a linear multivariate technique that has been frequently used in recent years both for diagnostics (Díaz et al. 1998; Nicholls 1987, among others) and predictability studies (Barnett and Preisendorfer 1987; Barnston and Ropelewski 1992; Shabbar and Barnston 1996, among others).

Bimonthly values of standardized precipitation anomalies were predicted during the period 1947–86 using SST data in the region 20°N–40°S, 150°E–80°W (244 grid points). Thus, 3-month SST averages were used to forecast the bimonthly rainfall anomalies at each station, with a 3-month lag period (e.g., the average SST field during July–September was used to anticipate the rainfall anomaly in January–February). The objective of this exercise is the assessment of the seasonal and spatial characteristics of seasonal rainfall predictability based on tropical Pacific SST.

The necessary preprocessing data needed as the input to CCA as used in this particular analysis are briefly described below. For each station, bimonthly rainfall time series were standardized by subtracting the long-term mean and dividing by the standard deviation. Neither SST nor precipitation series were detrended. Principal component analysis was used to reduce spatially redundant information, retaining p and q components for SST and rainfall, respectively, which account for 80% of the total variance in each of the fields. Depending on the bimonthly interval, p typically varied from 9 to 12, and q varied from 11 to 15. The CCA method yields orthogonal linear combinations of the predictand and predictor PC time series in a way to maximize the linear correlation between them. The r linear combinations [$r = \min(p, q)$] are called canonical component vectors (predictand and predictor). The reader is referred to Barnett and Preisendorfer (1987) and Graham et al. (1987a,b) for a detailed description of the method.

The skill of bimonthly rainfall predictions using CCA during the period 1947–86 was assessed using the cross-validation method (Michaelsen 1987). Then, to predict the rainfall anomalies of a selected bimonthly period for a specific year belonging to the 1947–86 period, a CCA model was built after removing from the predictor and predictand series the values corresponding to that year. This process was performed for all years in that period. The number of canonical component vectors used in the CCA model was selected as to maximize the predictability skill score.

The seasonal patterns of bimonthly predictability are analyzed using a measure of predictability skill, which corresponds to the percentage of correct hits in anticipating the rainfall tercile (dry, normal, or wet), called local skill (Barnett and Preisendorfer 1987). Terciles of predicted rainfall anomalies distribution are used to determine the predicted categories (dry, normal, or wet) and a binomial distribution is used to assess statistical significance.

Patterns of local skill are presented in Fig. 6. These patterns are quite similar to those in Fig. 3 describing the simultaneous SST–rainfall relationship. Significant levels of predictability are observed in central Chile during winter. In JJ the signal is restricted to the region around 31°S and extends to the whole of central Chile during JA. During fall and winter a significant predictability appears in the northern sector of Rio Grande do Sul, but it is only during JA that a significant simultaneous SST–rainfall relationship is observed (Fig. 3).

From winter to spring a southward shift of the region with significant skill scores is observed in Chile. The relatively weak predictability registered in Chile during SO, and elsewhere in subtropical South America, are probably due to the fact that the rainfall forecasts for this bimonthly interval are based on SST data during

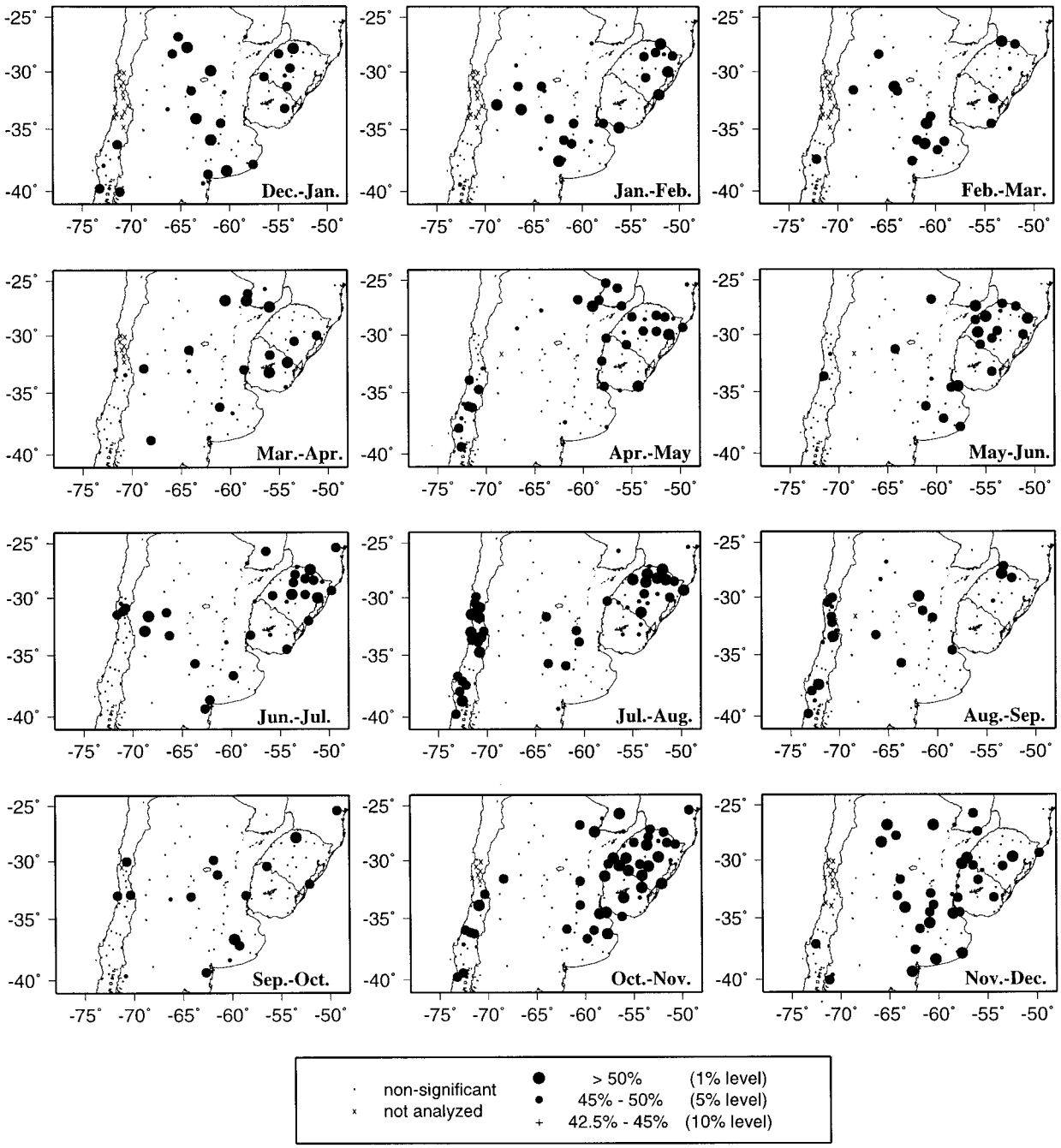

FIG. 6. Patterns of local skill (as described in the text) of bimonthly rainfall predictability, using tropical Pacific SST one season in advance. Sliding bimonthly intervals are DJ, JF, FM, up to ND. Symbols indicate different significant levels (see code in the figure).

the March–May trimester, when the SST interannual variance is at the minimum in the annual cycle (Table 3), and the air–sea interaction in the tropical Pacific is relatively weak (Zebiak and Cane 1987).

During spring and early summer the regions with significant rainfall predictability appear on the east side of the continent. Thus, in ON a coherent region with significant predictability skill includes southern Brazil, southern Paraguay, Uruguay, and eastern Argentina. During ND, an overall decrease in the level of predictability is noticed (particularly in southern Brazil) together with a displacement toward the west of the area of significant skill scores (similar to the shift experienced by the patterns of simultaneous correlation in Fig.

3). The westward displacement of the pattern continues in DJ, producing significant levels of predictability at stations in the central continental strip.

5. Discussion and conclusions

The simultaneous relationship between tropical Pacific SST and rainfall in subtropical South America and rainfall predictability one season ahead have been analyzed on a bimonthly basis using a variety of multivariate techniques (correlation, stratification, principal component, and canonical correlation analysis).

The simultaneous SST–rainfall relationship exhibits a marked seasonality and reaches significance in specific regions mostly located on the eastern and western sides of the continent. With a few exceptions, the relationship is of the warm–wet/cold–dry type. The stratification analysis suggests a more widespread impact of anomalously warm equatorial Pacific on rainfall compared with that when negative SST anomalies prevail. Moreover, the simultaneous SST–rainfall relationship is more significant during the second semester of the year when ENSO-related SST anomalies in the tropical Pacific reach their full strength and accordingly their influence on the global climate is highest.

A significant tendency is documented for positive (negative) rainfall anomalies on the western side of the continent (central Chile, 30°–35°S) during winter when anomalously warm (cold) conditions prevail in the equatorial Pacific. During the spring the region with a warm–wet/cold–dry relationship in Chile moves southward to the 35°–40°S latitudinal band. In summer, a tendency for rainfall deficit was documented for central–southern Chile during warm conditions in the central equatorial Pacific. The dynamic aspects of these SST–rainfall relationships are still a matter of further study. However, it is proposed that a larger frequency of blocking in the southeastern Pacific, combined with the seasonal displacement of the subtropical anticyclone in the South Pacific during the spring, could contribute to the southward shift of the warm–wet relationship from winter to spring.

The present study shows a clear shift of the warm–wet/cold–dry relationship from southeastern South America (SSA) in October–November toward a longitudinal band between 65° and 60°S in Argentina, during December–January.

Regarding the characteristics of the SST–rainfall relationship, it is worth noting that in the two regions with a highly significant warm–wet/cold–dry relationship, the ENSO-related rainfall anomalies are best defined after the maximum in the annual cycle of precipitation (JA in Chile and ON in the SSA; cf. Fig. 1). A similar behavior is observed in eastern Argentina where a significant SST–rainfall relationship appears in ND, following the maximum in the annual cycle in ON. To elucidate this matter, a deeper knowledge of the mechanisms controlling the annual cycle of precipitation in these regions is of paramount importance in order to improve the knowledge on the dynamics of rainfall interannual variability.

The study of the seasonality and spatial patterns of rainfall predictability in subtropical South America, based on tropical Pacific SST, shows that significant level of predictability in the majority of the cases is found in regions and bimonthly periods when a significant simultaneous SST–rainfall relationship exists. This is highly indicative that persistence of SST anomalies in the tropical Pacific is the main source of seasonal rainfall predictability, when SST is used as predictor.

Thus, a combined use of output from numerical and statistical models aimed at the forecast of SST anomalies in the equatorial Pacific with the simultaneous SST–rainfall relationship documented in this study can be used to anticipate plausible rainfall scenarios when anomalously warm or cold conditions are expected in the equatorial Pacific. It should be noticed that in cases when near-normal SST conditions are expected, the rainfall forecasts using this approach are highly uncertain, due to the fact that in those cases a weak tropical Pacific SST forcing of the extratropical circulation is expected. In fact, it was confirmed in this study that the distribution of rainfall categories (dry, normal, and wet) does not differ significantly from the climatology, when SST anomaly is within the range defined by the 20th and 80th percentiles.

When comparing patterns of predictability in Fig. 6 with Fig. 3 it was observed that significant levels of predictability also appear in areas where the simultaneous SST–rainfall relationship is relatively weak. This situation appears in southern Brazil, southern Paraguay, and Uruguay where the predicted rainfall anomalies in fall and winter (MA, AM, MJ, and JJ) could be related to the positive (negative) rainfall anomalies that Pisciottano et al. (1994) described for March–July of year +1 of El Niño (La Niña) events for Uruguay. In this specific case, the persistence of the tropical Pacific SST does not appear to be the source of predictability. In this respect, it is worth pointing out the results of Díaz et al. (1998), who documented the existence of a simultaneous relationship between rainfall in SSA and SST anomalies in the southwestern Atlantic during fall and winter. It deserves further investigation whether delayed SST anomalies linked to ENSO in this region could be at the origin of rainfall predictability in SSA at this time of the year.

Acknowledgments. We wish to thank N. Nicholls, C. R. Mechoso, and an anonymous reviewer for their constructive comments. This work was mainly supported by Grant Fondecyt 1961110 and Grant FONDEF 97-2028 of CONICYT-Chile and Grant 96-62 of the Pan American Institute of Geography and History. A.D. acknowledges the support of CONICYT-Uruguay (Project 117/94) and of IAI (Cooperative Agreement ATM-9209181, Subaward UCAR S97-74046, UCAR/UR).

REFERENCES

Aceituno, P., 1988: On the functioning of the Southern Oscillation in the South American sector. Part I: Surface climate. *Mon. Wea. Rev.,* **116,** 505–524.

Barnett, T. P., and R. W. Preisendorfer, 1987: Origins and levels of monthly and seasonal forecast skill for United States surface air temperatures determined by canonical correlation analysis. *Mon. Wea. Rev.,* **115,** 1825–1850.

Barnston, A. G., and C. F. Ropelewski, 1992: Prediction of ENSO episodes using canonical correlation analysis. *J. Climate,* **5,** 1316–1345.

Díaz, A. F., C. D. Studzinski, and C. R. Mechoso, 1998: Relationships between precipitation anomalies in Uruguay and southern Brazil and sea surface temperature in the Pacific and Atlantic Oceans. *J. Climate,* **11,** 251–271.

Feller, W., 1957: *An Introduction to Probability Theory and its Applications.* 2d ed. Vol. 1, John Wiley and Sons, 461 pp.

Graham, N. E., J. Michaelsen, and T. P. Barnett, 1987a: Investigations of the El Niño Southern Oscillation with statistical models. Part 1: Predictor field characteristics. *J. Geophys. Res.,* **92,** 14 251–14 270.

——, ——, and ——, 1987b: Investigations of the El Niño Southern Oscillation with statistical models. Part 2: Model results. *J. Geophys. Res.,* **92,** 14 271–14 290.

Grimm, A. M., S. E. Ferraz, and J. Gomes, 1998: Precipitation anomalies in southern Brazil associated with El Niño and La Niña events. *J. Climate,* **11,** 2863–2880.

Kiladis, G., and H. Díaz, 1989: Global climatic anomalies associated with extremes in the Southern Oscillation. *J. Climate,* **2,** 1069–1090.

Lau, N.-C., and M. J. Nath, 1994: A modeling study of the relative roles of tropical and extratropical SST anomalies in the variability of the global atmosphere–ocean system. *J. Climate,* **7,** 1184–1207.

Michaelsen, J., 1987: Cross-validation in statistical climate forecast models. *J. Climate Appl. Meteor.,* **26,** 1589–1600.

Nicholls, N., 1987: The use of canonical correlation to study teleconnections. *Mon. Wea. Rev.,* **115,** 393–399.

Pisciottano, G. J., A. F. Díaz, G. Cazes, and C. R. Mechoso, 1994: El Niño–Southern Oscillation impact on rainfall in Uruguay. *J. Climate,* **7,** 1286–1302.

Pittock, A. B., 1980: Patterns of climatic variation in Argentina and Chile. Part I: Precipitation, 1931–1960. *Mon. Wea. Rev.,* **108,** 1347–1361.

Quinn, W., and V. Neal, 1983: Long-term variations in the Southern Oscillation, El Niño and the Chilean subtropical rainfall. *Fish. Bull.,* **81,** 363–374.

Rasmusson, E. M., and T. H. Carpenter, 1982: Variations in tropical sea surface temperature and surface wind fields associated with the Southern Oscillation/El Niño. *Mon. Wea. Rev.,* **110,** 354–384.

Reynolds, R. W., and T. M. Smith, 1994: Improved global sea surface temperature analyses using optimum interpolation. *J. Climate,* **7,** 929–948.

Ropelewski, C. F., and M. S. Halpert, 1987: Global and regional scale precipitation patterns associated with El Niño–Southern Oscillation. *Mon. Wea. Rev.,* **115,** 1606–1626.

——, and ——, 1989: Precipitation patterns associated with the high index phase of Southern Oscillation. *J. Climate,* **2,** 268–284.

Rubin, M. J., 1955: An analysis of pressure anomalies in the Southern Hemisphere. *Notos,* **4,** 11–16.

Rutllant, J., and H. Fuenzalida, 1991: Synoptic aspects of the central Chile rainfall variability associated with the Southern Oscillation. *Int. J. Climatol.,* **11,** 63–76.

Shabbar, A., and A. G. Barnston, 1996: Skill of seasonal climate forecasts in Canada using canonical correlation analysis. *Mon. Wea. Rev.,* **124,** 2370–2385.

Trenberth, K. E., 1997: The definition of El Niño. *Bull. Amer. Meteor. Soc.,* **78,** 2771–2777.

Wright, P. B., 1989: Homogenized long-period Southern Oscillation indices. *Int. J. Climatol.,* **9,** 33–54.

Zebiak, S. E., and M. A. Cane, 1987: A model El Niño–Southern Oscillation. *Mon. Wea. Rev.,* **115,** 2262–2278.